Load testing of large diameter single drilled shaft foundations for the REM project in Montreal

R. Diab, L. D'Amours & D. Zirmi
SNC-Lavalin, Montreal, Quebec, Canada

J. Habib
Englobe Corp., Montreal, Quebec, Canada

ABSTRACT

In 2018, the Caisse de Dépôt et Placement du Québec (CDPQ) awarded a $6.3 Billion Design-Build contract to the Joint Venture (JV) team NouvLR (led by SNC-Lavalin) for the design and construction of the Réseau Express Metropolitain (REM) in Montreal. Out of the 67 km network, over 25 km will be constructed on an elevated structure founded on single drilled shafts socketed into rock. In order to optimize the design and allow the use of higher resistance values, the JV team performed two full-scale, bidirectional (Osterberg Cell) static load test in two of the rock formations encountered along the alignment.

This paper presents design details on the back-calculated side and base resistance values, a discussion on the displacement incompatibility of skin and end resistance. Equivalent load-settlement curve developed based on the load tests is presented to illustrate the overall shaft capacity within a displacement-based design framework.

RÉSUMÉ

En 2018, la Caisse de dépôt et placement du Québec (CDPQ) a confié à NouvLR le contrat d'ingénierie, d'approvisionnement et de construction des infrastructures du Réseau express métropolitain (REM). Un contrat de 6,3 milliards dollars, pour un réseau de 67 km avec plus de 25 km qui seront construits sur des structures surélevées reposant sur des caissons avec emboîture au roc. Afin d'optimiser la conception des fondations, l'équipe conception a réalisé deux essais de chargement statique bidirectionnels (Osterberg Cell) dans deux types de roches rencontrées le long du tracé.

Cet article présente les détails de conception sur les valeurs de résistance latérale et de résistance en pointe calculées à partir des résultats des essais, ainsi qu'une discussion sur l'incompatibilité des déplacements mobilisé aux frottements le long du fut et la résistance en pointe. Une courbe charge-déplacement développée à partir de l'essai de chargement est présentée pour illustrer la capacité du caisson basé sur les déplacements dans un cadre de conception.

1 INTRODUCTION

Réseau Électrique Métropolitain (REM) is being constructed by a joint venture, NouvLR, comprised of SNC Lavalin, Dragados Canada, Groupe Aecon Quebec, Pomerleau, and EBC, partnering with Aecom and SNC Lavalin as the lead design firms. The project, referred to as REM, is a fully automated light rail transit (LRT) proposed by the Caisse de dépôt et placement du Quebec (CDPQ) Infra, to serve the major metropolitan areas in Montreal, Canada. Once completed, the 67 km REM will be one of the largest automated transportation systems in the world and will represent the largest public transportation infrastructure for the metropolitan area since the Montreal metro, inaugurated in 1966.

As shown on Figure 1 below, the new facility will link downtown Montréal, South Shore, West Island (Sainte-Anne-de-Bellevue), North Shore (Deux-Montagnes), and the Montreal-Pierre Elliott Trudeau International Airport.

The project comprises four segments: South Shore (SS) segment with a total length of 15 km will extend from downtown (Central Station) to the DIX30 commercial district passing across to Nuns' Island and then will use a rail deck constructed on the new Champlain Bridge (still under construction) to cross the St. Lawrence River. Over 3.5 km will be supported by an elevated structure.

Figure 1. REM project alignment

The Deux Montagnes (DM) segment will be mostly at grade and will consist of a direct conversion of the existing Deux-Montagnes line.

The Sainte-Anne-De-Bellevue (SADB) segment will begin near highway A-13 and end at SADB with 17 km of elevated structure supported by two abutments and 340 piers.

The airport segment will divert from SADB line to make a stop in Technoparc St-Laurent before terminating at Montréal–Pierre Elliott Trudeau International Airport. The airport segment will include approximately 1 km of elevated guideway consisting of 2 abutments and 21 piers.

Several foundation alternatives have been evaluated for the structures and it was concluded that the most cost effective and reliable foundation system is single drilled shafts, socketed into sound rock. Depending on the loading conditions, the proposed drilled shafts will range from 2.0 m to 3.2 m in diameter with embedment of up to 9.0 m within the sound rock.

Generally speaking, drilled shafts constructed to bear on or within rock provide an extremely reliable foundation system due to the ability of the designer to observe and verify both the bearing stratum and the structural integrity of each drilled shaft foundation. Individual drilled shafts in rock are capable of supporting extremely high design loads, sometimes approaching the structural capacity of the reinforced column itself.

The advantage of using single shaft support is to avoid the need for a pile cap with the attendant excavation and temporary support or shoring system, a feature that could be important where new foundations are constructed near existing structures. However, the disadvantage is the lack of foundation redundancy. Failure of one foundation element may lead to an entire structure collapse.

As per the client (CDPQ) requirements, the design standards to be used for the geotechnical engineering design are the Canadian Highway Bridge Design Code (CSA-S6-14), the Canadian Foundation Engineering Manual (CFEM 2006), and AASHTO LRFD Bridge Design Specifications (8th Edition, 2017), in decreasing order of precedence.

2 SITE GEOLOGIC CONDITIONS

The general geology of the layout consists of a till deposit overlying the bedrock at varying depths (2 to 17 m). The surface of the bedrock is altered and fractured for depths varying from 1 to 3 m. Three rock types are encountered along the REM alignment. Limestone and dolomite are the main rock formations along DM and SADB. Shale is the only rock type along the SS segment.

3 OBJECTIVES

In order to optimize the geotechnical design and allow the use of higher resistance values for axial capacity, the JV team (NouvLR) agreed on performing one full-scale bidirectional (Osterberg Cell) static load test in each of the rock formations encountered in the project, namely limestone, dolomite and shale. However, since an O-cell test had already been performed for the new Champlain Bridge project (also designed and constructed by a Joint Venture led by SNC Lavalin) in shale, an authorization from the Champlain Bridge project Joint Venture (Signature Saint-Laurent, SSL) to obtain and use the results was awarded. As a result, NouvLR performed one load test in dolomite and the other in limestone. The purpose of the tests was to determine the design values of side and base resistance at the ultimate limit state on a drilled shafts constructed using means and methods which are identical to those to be used on production foundations. The results and analysis of the two load tests are presented in this paper. The results of the O-cell performed in shale will not be presented as an authorization from SSL has not been obtained at this point.

The other objective of the load test is the development of an equivalent top load-settlement curve for production piles, calibrated with the results of the load tests. Such a curve will be used basically for settlement estimate at the serviceability limit state. The construction of the load-settlement curve is presented in this paper.

4 SUBSURFACE INVESTIGATION

The design-phase investigation included one boring per substructure. All of the borings included a minimum of 10 m of rock coring but in no case less than 5 m below the pre-determined shaft tip elevation.

The dominant bedrock encountered along the SADB and DM alignments was hard, gray, very finely crystalline, medium to massive bedded, fresh limestone although some thin shale layers in the order of 12 to 50 mm were occasionally observed. In some areas within the DM segment and in the section close to the SADB Station, the rock was described as dolomite. No cavities or sinkhole activities were noted within the limestone and dolomite during the investigation and therefore, the potential for solution cavities was not a concern for the project.

Intensive soil and rock investigation was performed at the load test locations, which included SPT borings, pressuremeter (in soil) and dilatometer (in rock), and Nilcon vane shear test in cohesive soil. The pressuremeter and dilatometer models used for the testing were the Texam model and the Probex model respectively. The laboratory program consisted basically of sieve and hydrometer analysis of soils and unconfined compressive tests and elastic modulus of rock.

At the SADB load test location, the borings indicated that the overburden soil consist of an upper 4.4 m of clayey silt deposit with an average undrained shear strength measured in the field with Niclon vane shear test of 57 kPa, underlain by a layer of glacial till consisting mainly of very dense silty sand and gravel.

The bedrock surface was comprised of poor quality, weathered metamorphosed conglomerate with some calcite veins which extended from a depth of 11.4 to 12.1 (elevations 15.47 to 14.78 m). The RQD of the upper part of this rock was noted to be 25 percent. Below the meta-conglomerate was dolomite that extended to the base of the borehole and ranged from poor to good quality with an average RQD of 69 percent.

At the DM load test location, the drilled borings indicated that the upper 3 m of the overburden consist of fill material containing predominantly silt and sandy silt with an average SPT ‘N’ value of 4 blows/0.3 m, underlain by about 4 m layer of glacial till consisting of silty sand with an average SPT ‘N’ value of about 14 blows/0.3 m.

The rock was encountered at depth of 7 m and consisted of grey limestone. The upper 0.75 m was of bad

quality with an RQD of 22. The bottom rock was good to excellent quality with an average RQD of 83 percent.

A thorough examination of the rock quality through which the tested drilled shafts were constructed shows the following rock parameters:

Table 1. Rock Parameters

Parameters	SADB	DM
Rock type	Dolomite	Limestone
Average RQD along the shaft	67 percent	83 percent
Average joint modification factor, α	0.72	0.82
Average intact rock modulus, E_i	75.6 GPa	56.7 GPa
Average dilatometer modulus, E_d[1]	12.2 GPa	12.7 GPa
Poisson ratio, μ	0.33	0.29
Average rock unconfined compressive strength, q_u	145 MPa	68 MPa
Coefficient of discontinuity spacing, K_{sp}	0.20	0.20
Geologic Strength Index, GSI	59	61

[1]As obtained from dilatometer tests

5 CONSTRUCTION PROCEDURE

A 1,300 mm diameter permanent steel casing was placed at the proposed location. A hydraulic rig (LB 36-410) was used to insert the casing through the overburden and the fractured rock until refusal on the rock surface was reached. The overburden was excavated with an auger mounted on the drilling equipment.

Once the casing had been sealed into rock, an auger and a bucket were used for drilling a 1,180 mm shaft socket with a minimum of 300 mm of recess. To obtain a relatively flat base on the rock surface, the sub-contractor used a cleaning bucket (KBF-K) to flatten the surface. Figure 2 shows the placement of the casing and the soil excavation.

The bottom and the rock socket walls of the shaft were cleaned with an airlift multiple times. The following cleanout criteria were met:

- Maximum depth of sediment or any debris at any place on the base of the shaft not to exceed 40 mm.
- Average depth of sediment is less than 15 mm of sediment at the time of concrete placement.

After cleaning the base, the frame with the attached O-cell assembly was inserted into the excavation and temporarily supported from the outer steel casing. Crosshole Sonic Logging (CSL) tubes were attached to the interior of the reinforcement cage. A photograph of the frame and the O-cell assembly is provided in Figure 3. The tremie pipe was then placed through the tremie hole.

The concrete was pumped through a 5-inch diameter O.D. tremie line into the base of the shaft. During the concrete pouring, the volume of concrete in the pile was monitored as well as the volume that was poured from the delivery trucks combined with the concrete elevation which was measured on site directly

Figure 2. Casing placement and soil excavation

into the shaft. The tremie pipe was held at least 3 meters in concrete at all times.

The constructed drilled shafts were subjected to multiple levels of quality control measures. Open shaft verticality through overburden soils was measured by the drilling rig alignment control and with the help of a 1.2 meters long spirit level for each shaft. This confirmed shaft verticality of the order of 0 - 2% was achieved. Once rock socket drilling was completed a Sub-Camera inspection device was used to confirm the rock socket base cleanliness using five spot sediment checking criteria. Then, construction quality control involved concrete integrity testing using Ultrasonic Crosshole Testing (CSL) and pile integrity testing.

6 LOAD TEST RESULTS

The bi-directional static O-cell load tests on full-scale non-production test shafts were performed by LoadTest, Inc, on July 9 and 12, 2018 for SADB and DM segments,

respectively in accordance with ASTM D1143 Loading Procedure A – Quick Test. The tests were performed using one (1) 13.8 MN bidirectional embedded jacks (O-cell) to load the base area of the shaft against the side resistance of the socket above the base.

Figure 3. Rebar cage & load tests assembly

The concept known as the “Chicago Method”, which consists of utilizing a smaller base area to maximize the unit base pressure, was used. This approach is particularly effective in testing shaft with limited rock socket embedment. Since the bottom plate O-cell was smaller than the upper one and much smaller than the shaft socket (See Table 2 below), the base resistance acted against a 720 mm diameter area and the side shear reaction acted against a 1,180 mm diameter socket. A larger unit end bearing pressure was thus mobilized by utilizing a larger diameter socket for side shear reaction.
At the maximum load, the displacements above and below the O-cell were 3.56 mm and 9.58 mm, respectively in dolomite (SADB); and 2.04 and 14.18 mm, respectively in limestone (DM). Those displacements correspond to maximum downward and upward loads of 20.53 and 20.18 MN, respectively in dolomite (SADB); and 20.56 and 20.21 MN, respectively in limestone (DM). The upward load represents the net load which is defined as gross O-cell load minus the buoyant weight of the pile above. The tested drilled shaft properties are shown on Table 2 below.

Table 2. Drilled Shaft Properties

Characteristics	SADB	DM
Nominal pile diameter in soil and fractured rock	1,300 mm	1,300 mm
Nominal pile diameter in sound rock	1,180 mm	1,180 mm
Length of pile below the base of O-cell:	100 mm	130 mm
O-cell top plate diameter	880 mm	880 mm
O-cell bottom plate diameter	720 mm	720 mm
Assumed concrete unit weight	2,322 kg/m^3	2,322 kg/m^3
Concrete compressive strength on the day of the test	47.4 MPa	41.4 MPa
Assumed concrete elastic modulus	33,104 MPa	30,936 MPa
Pile tip elevation	11.65 m	19.49 m
Bottom of permanent casing elevation	14.75 m	22.59 m
Maximum bi-directional load applied to the pile	20.53 MN	20.56 MN

The load-displacement curves for SADB and DM are shown in Figures 4a and 4b. Since the bottom O-cell plate was located slightly above the shaft base (See Table 2), the measured unit base resistance provided in the figure from the two test shafts were based on the projected area from the base plate plus a distribution of 2(vert):1(horiz) downward through the 100 mm at SADB and 130 mm at DM of concrete below the base plate.

Four levels of two sister bar vibrating wire strain gages were attached diametrically opposed to the reinforcing cage. Two of the levels (Levels 1 and 2) were in the rock socket area below the steel casing. Figure 5 shows the calculated unit skin friction versus pile vertical displacement in Zones 1 and 2 of the test pile, where Zone 1 is defined between the O-cell and strain gages in Level 1 and Zone 2 is located between the strain gages in Levels 1 and 2. The results showed that the skin friction in the zones within the steel casing (soil and fractured rock) was negligible compared to the unit skin friction developed along the rock socket. Hence, the skin friction along the steel casing was neglected in subsequent analyses and recommendations, assuming that for the production pile steel casing penetrates through overburden soil and the fractured rock.

Since the bottom O-cell plate (just above the shaft base) is significantly smaller than the shaft base area, the scaling effect was considered to develop the displacement versus unit end bearing curves. For this perspective, the theory of elasticity was used to estimate the displacement of the entire pile base area (1.09 m^2) associated with the pressure applied at the bottom O-cell plate (0.41 m^2). In other words, the displacement that would occur at the pile tip was calculated as if the stresses at the bottom plate were applied over the entire base area.

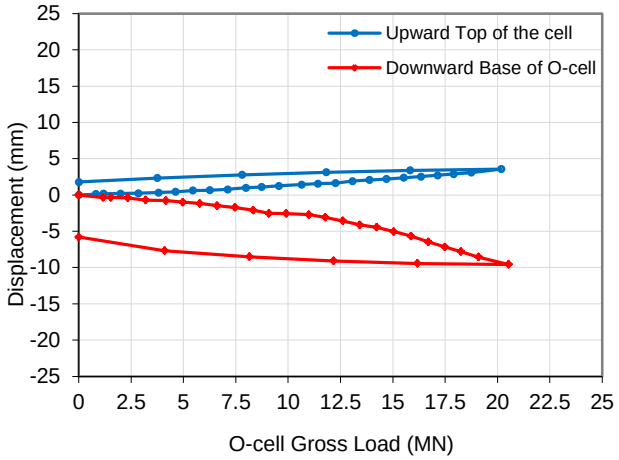

Figure 4a. O-cell Load-Displacement Curves in Dolomite

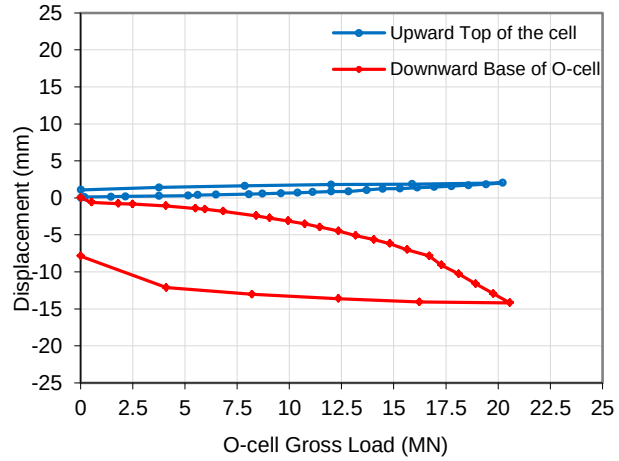

Figure 4b. O-cell Load-Displacement Curves in Limestone

Figures 6a and 6b present the pile tip displacement versus the measured unit end bearing as well as the corrected (modified) end bearing estimated for the full base when the same pressure is applied, for dolomite and limestone. The mobilized skin friction curves are plotted on the same figures.

7 DESIGN IMPLICATIONS

Major factors affecting the design of the foundation at the REM bridges included lateral and overturning forces from wind, collision forces, and seismic demands. A design decision was thus made to socket all shafts a minimum of one diameter into sound rock to provide lateral stability. As a result, all drilled shafts were socketed a minimum of 2 m into rock. In general, drilled shafts socketed in rock and subject to compressive loading are designed either in skin friction on the wall of the rock socket, end bearing on the material below the tip of the drilled shaft, or a combination of both. A decision by REM geotechnical team was made to design the drilled shafts such that both the toe and side resistance are to be used for estimating socket capacity.

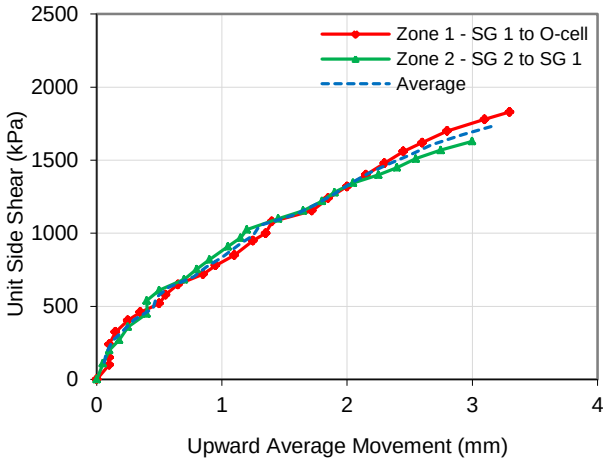

Figure 5a. Mobilized unit skin friction vs displacement in dolomite (SADB Segment)

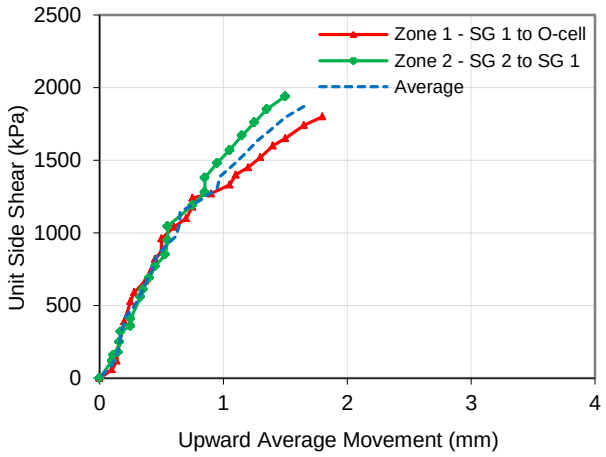

Figure 5b. Mobilized unit skin friction vs displacement in limestone (DM Segment)

7.1 Skin Friction

A typical design approach for side resistance relates the unit side resistance, f_s and the square root of the unconfined compressive strength of the bedrock, $\sqrt{q_u}$. The method contained in Turner (2006) originally dating back to Horvath and Kenney (1979), and normalized to dimensionless units is presented as equation (1):

$$f_s = C.P_a.\sqrt{\frac{q_u}{P_a}} \quad [1]$$

Where P_a is the atmospheric pressure (101 kPa), C is an empirical constant and q_u is the unconfined compressive strength of the rock. In general, the lesser of the compressive strength of either the concrete or rock is used for design.

The current edition of AAHTO 2017 recommends the use of a value of 1 for the parameter C, based on the most recent regression analysis of available load test data that is reported by Kulhawy et al. (2005) and that

demonstrates that the mean value of the coefficient *C* is approximately equal to 1.0. A lower bound value of *C* = 0.63 was shown to encompass 90% of the load test results. The Canadian Foundation Engineering Manual (CFEM) 2006, on the other hand, recommends a range of values between 0.63 and 1.41 reflecting the variability of test results obtained by different authors.

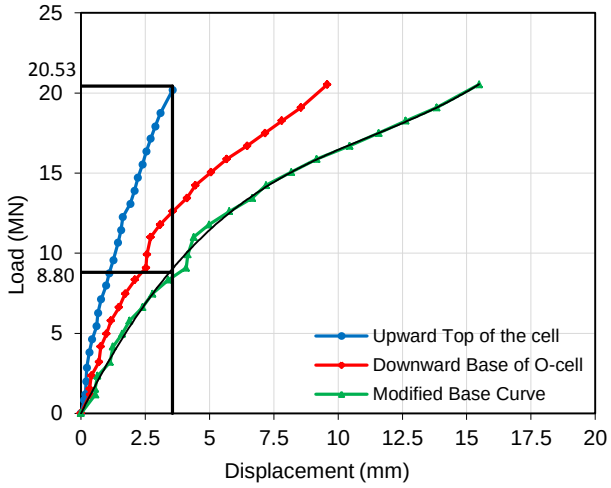

Figure 6a. Skin Friction and End Bearing from O-cell Test at SADB (dolomite)

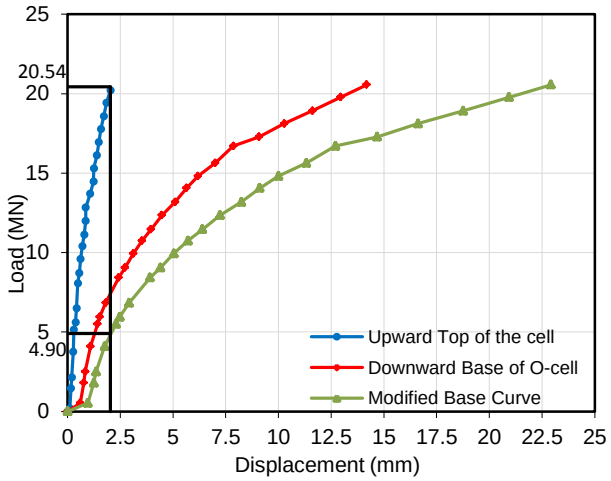

Figure 6b. Skin Friction and End Bearing from O-cell Test at DM (limestone)

One of the objectives of the load test was to calibrate the empirical parameter *C* against the results of the O-cell test, at the project site for both limestone and dolomite.

The data on Figures 4 through 6 shows the maximum unit skin friction mobilized during the test along the rock socket is 1.80 MPa for dolomite (SADB) and 1.87 MPa for limestone (DM). Based on these input values, a value of *C* equal to 0.82 at SADB and 0.92 at DM was back-calculated from the equation above. These values of *C* generally agree with other load tests performed in limestone and dolomite (Brown, 2008).

It should be noted that the average unconfined compressive strength of the rock, q_u, at the site was 145 MPa and 68 MPa for dolomite and limestone respectively. Thus the strength of the rock substantially exceeded the 47.4 and 41.4 MPa compressive strength of the concrete used for the drilled shaft. As a result, the value of concrete compressive strength was substituted for q_u in the above equation.

Moreover, it is important to note that the maximum measured side resistance was less than the nominal (ultimate) strength value due, most likely, to the fact that the concrete compressive strength on the day of testing was higher than the anticipated design concrete strength of 35 MPa. Therefore, any back-correlation using the measured values represents a lower bound value since the test was limited by the capacity of the system, and failure was not attained. For the purpose of the analysis, the maximum mobilized unit skin friction was, conservatively, considered as the ultimate unit skin friction for this rock stratum. Thus, considering the ultimate resistance was not attained the value of *C* for both tests approaches unity as recommended by AASHTO.

7.2 Base Resistance

The base resistance of the two tested shafts was mobilized at relative displacements (percent of vertical displacement divided by shaft diameter) of just over 1% of the diameter of the shaft, but did not mobilize the geotechnical limit of the rock formation in terms of bearing capacity.

The ultimate end bearing is given by the following equation, as recommended by the CFEM (2006):

$$q_t = 3.K_{sp}.q_u.d \qquad [2]$$

Where K_{sp} is the coefficient of discontinuity spacing which is a function of both spacing and aperture of rock discontinuities and *d* is a depth factor = 1+0.4 (L/D) ≤ 3.

The latest edition of AASHTO, on the other hand, recommends the following relationships between the nominal unit base resistance and the compressive strength of the rock. Equations (3) and (4) are for intact and jointed rock respectively.

$$q_t = N_{cr}.q_u \qquad [3]$$

$$q_t = A + q_u\left[m_b\left({}^{A}/_{q_u}\right) + s\right]^a \qquad [4]$$

Where m_b, *s*, and *a* are the Hoek-Brown strength parameters and N_{cr} is an empirical bearing capacity factor for rock. A value of 2.5 for N_{cr} is recommended by AASHTO based on studies reported by Prakoso and Kulhawy (2002).

The average q_u of the rock beneath the base of the test shaft was about 145 MPa for dolomite (at SADB) and 48.5 MPa for limestone (at DM). Therefore, using either of the equations above leads to unit base resistance (q_t) values of about 175 and 60 MPa for dolomite (SADB) and limestone (DM), respectively, which largely exceeds the maximum measured unit base resistance in the load test of about 19 MPa in both cases. In other word, the

mobilized end bearing was well below the nominal unit base resistance.

7.3 Tip Resistance Contribution

It is well documented in the literature and confirmed by the load test results that the end bearing resistance mobilizes at much larger displacements than the displacement required to mobilize skin friction. Generally speaking, the end bearing is fully mobilized at a relative displacement of about 3 to 5 percent of the diameter of the loaded area whereas the skin friction is fully mobilized at a displacement of about 10 mm. Therefore, the total ultimate axial resistance of a drilled shaft socketed into rock corresponds to mobilization of the full available side resistance plus a fraction of the available base resistance.

The O-cell test results showed that approximately 8.8 MN for dolomite (SADB) and 4.9 MN for limestone (DM) in end bearing were mobilized at the vertical displacement at which maximum skin friction was mobilized (see Figure 6). Thus approximately 30 percent of the total resistance (29.3 MN) for dolomite (SADB) and 19 percent of the total resistance (25.1 MN) for limestone (DM) were provided by the end bearing at displacements corresponding to maximum mobilized skin friction.

7.4 Load-Displacement Curve

The equivalent top-loaded load-displacement curve was constructed, basically for settlement estimation at the serviceability limit state, by summing the loads recorded in side and in end resistance corresponding to the same upward and downward movement, respectively. This procedure was followed point by point up to the maximum recorded side shear load. Since the end bearing movement was much larger than the skin friction movement, the side shear curve was extrapolated using hyperbolic curve fitting technique, which is well accepted in practice. Figure 7 shows the constructed load-settlement for the load test in limestone (DM). Similar load-displacement (not included) was constructed for dolomite.

8 CALIBRATION OF AXIAL RESISTANCE FOR OTHER LOCATIONS

8.1 Skin friction

In order to estimate ultimate unit skin friction in other locations along the REM alignment, where the same rock formation is encountered but where the rock is of different (lower or higher) quality, the joint modification factor, α, which is a function of RQD and joint type (i.e., open vs. closed) is introduced into Equation (1) above as shown in Equation (5). Values of α were selected using the guidelines presented in Table 3 taken from AASHTO (2017) Table 10.8.3.5.4b-1- (O'Neill and Reese,1999).

$$f_s = C_1.\alpha.P_a.\sqrt{\frac{q_u}{P_a}} \qquad [5]$$

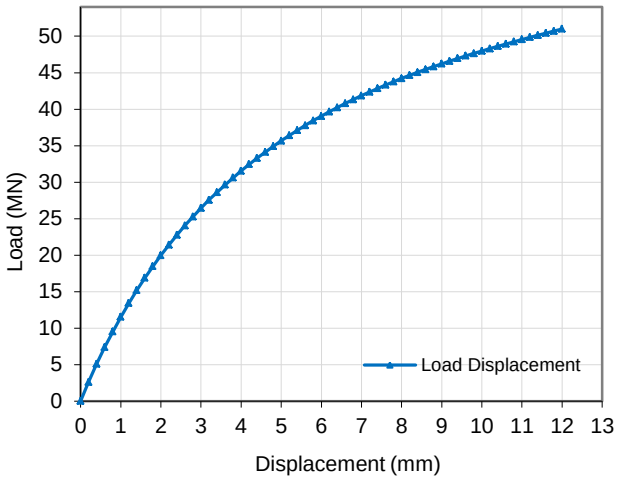

Figure 7. Skin Friction and End Bearing from O-cell Test at SADB

Where C_1 represents the ratio of C (0.82 for dolomite and 0.92 for limestone) to the value of α at the load test location (0.72 at SADB (dolomite) and 0.82 and DM (limestone)). Therefore the following values of C_1 are being used in the analysis:

- C_1 = 1.14 for dolomite (SADB)
- C_1 = 1.12 for limestone (DM)

Table 3. AASHTO Guidelines for Joint Modification Factor

	Joint Modification Factor, α	
RQD (%)	Closed Joints	Open or Gouge filled Joints
100	1.00	0.85
70	0.85	0.55
50	0.60	0.55
30	0.50	0.50
20	0.45	0.45

In summary, the skin friction is scaled down or up proportional to the ratio of α of the rock at a specific site location along the REM alignment to the value of α obtained for the rock at the load test location. In other terms, for areas where the rock has higher (or lower) quality with joint modification factor higher (or lower) than the rock quality at the load test location, the unit side friction is multiplied by the ratio α at the proposed site to α at load test location.

8.2 Tip Resistance Contribution

For the purpose of optimization, the production drilled shafts are being designed such that the nominal axial compression resistance is derived from both the tip and the side (skin) friction, assuming that both the concrete and rock behave as elastic isotropic solids and that the bonds between the rock and the concrete along the shaft are not broken. Therefore, the proportion of the load

reaching the base for productions piles, where the shaft diameters and socket lengths are different and where the rock quality could be different from the rock quality at the load test locations, must be estimated. To estimate the tip contribution to the total ultimate axial capacity, the displacement incompatibility of skin friction and end bearing was considered.

As mentioned above, the O-cell test results showed that approximately 19 percent for limestone (DM) and 30 percent for dolomite (SADB) of the total resistance was provided by the end bearing at displacements corresponding to maximum mobilized skin friction.

The CFEM (2006) recommends the use of the Pells and Turner (1979) approach to estimate the tip contribution. As expected, the longer the embedment depth into sound rock (rock socket), the smaller the load reaching the socket base. Also, the smaller the ratio of concrete modulus to rock mass modulus E_c/E_r, the smaller the tip resistance contribution.

At the load test locations where the ratio of *L/r* was equal to 5.2 and E_c/E_r was equal to 2.7 in dolomite and 2.4 in limestone, the Pells and Turner approach shows that approximately 8 percent of the total resistance would be taken by the end bearing for both limestone and dolomite.

In order to optimize and calibrate the tip resistance contribution for different *L/r* ratios and different rock qualities, the load test results were used to plot the best estimate curve for E_c/E_r=2.7 (dolomite) and 2.4 (limestone) on the Pells and Turner graph, as shown on Figures 8a and 8b below (red curves). The curves were multiplied by a factor equal to 0.7 to introduce a margin of safety. Based on the load test calibrated curve (red curves), the tip resistance contribution for limestone for *L/r* of 2, 4, and 6 would be 33, 16, and 11 percent whereas the tip contribution estimated based on the Pells and Turner approach (green curve on Figure 8) would be 27, 11 and 7 percent, respectively. As for dolomite, for the same *L/r* ratios the tip resistance contribution, based on the load test plotted curve, would be 44, 26, and 20 percent whereas the tip contribution estimated based on the Pells and Turner approach would be 25, 10 and 5 percent, respectively.

Therefore, for the purpose of optimizing the design and estimating the tip resistance contribution for production shafts, where the rock could be of different (lower or higher) quality and where the ratio of *L/r* could be different, the tip resistance obtained from Pells and Turner curves could be multiplied by an adjustment factor equal to:

Limestone

- 1.2 for *L/r* = 2
- 1.4 for *L/r* = 4
- 1.6 for *L/r* = 6

Dolomite

- 1.75 for *L/r* =2
- 2.60 for *L/r* =4
- 4.0 for *L/r* = 6

Linear interpolation could be used for different *L/r* ratio.

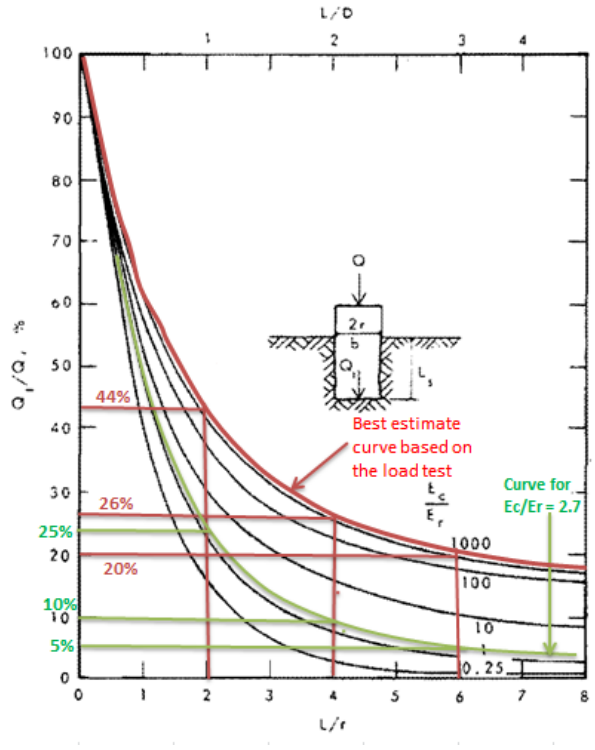

Figure 8a. Design Load Distribution in a Rock Socket for dolomite (SADB)

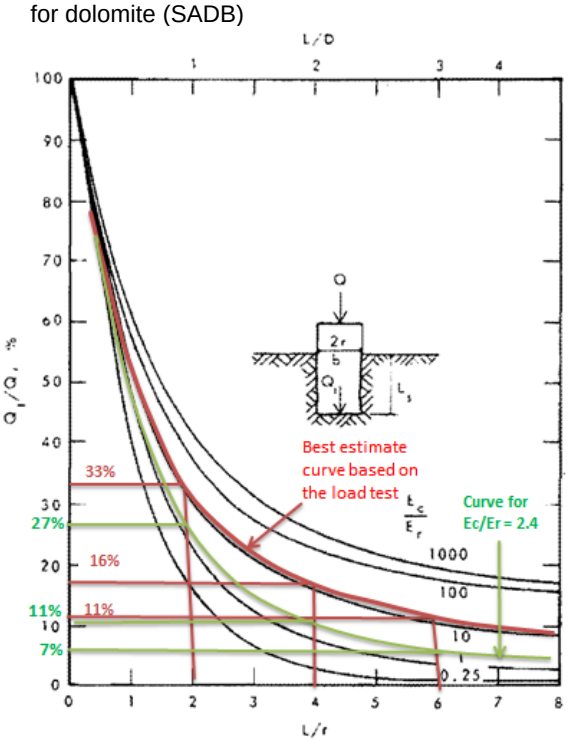

Figure 8b. Design Load Distribution in a Rock Socket for limestone (DM)

It is of interest to mention that the magnitude of load transferred to the tip based on Kulhawy and Carter (1992) approach discussed in the FHWA publication compares

relatively well with the load test results, particularly within the linear elastic portion.

It should be emphasized that thorough cleaning of the bottom shaft is crucial for the development of end bearing. The allowed tolerances used for the construction of the tested shafts and subsequent production shafts were as follows:

- A minimum of 50 percent of the base of the shaft shall have less than 15 mm of sediment at the time of concrete placement.
- The maximum depth of sediment or any debris at any place on the base of the shaft shall not exceed 40mm.

8.3 Load-settlement Curve

In order to calibrate the load-settlement curve for other locations where the rock conditions and shaft diameters are different, the closed-form solutions proposed by Kulhawy and Carter (1992) was used. According to the solution, the skin friction in rock socket develops through shearing of bond between the concrete and the rock (bond), sliding friction between concrete shaft and rock (friction), and dilation of an unbounded rock-concrete interface (dilation). As a result, the load-displacement curve consists of linear elastic portion when relatively small loads are applied and where the shaft behavior is controlled by the elastic parameters of the rock and the concrete, followed by a transition zone through which the socket bonds begin to rupture and then a third portion, representing the full slip, when the entire shaft will slip. At this point, a great portion of the total axial load is transmitted to the tip. The full slip behavior is controlled basically by three parameters, namely the rock-concrete cohesion, c, rock-concrete friction angle, φ, and the angle of dilation ψ. By trial and error, different combination of c, φ, and ψ were introduced into the Kulhawy and Carter model until the resulting load-settlement curve had a good match with the load test load-settlement curve (Figure 7). The values of c, φ, and ψ were found to be equal to 1.4 MPa, 26 degrees, and 1.2 degrees, respectively. Figure 9 below shows the normalized load-settlement curve as obtained by the Carter and Kulhawy model. As can be seen, for design purposes, the transition zone was ignored and the initial linear elastic response and the full slip condition were considered representative of the overall shaft behavior. A spread sheet was prepared to develop the load settlement curve for different rock qualities and different shaft diameters using the above mentioned parameters. It should be emphasized that these parameters depend largely on the construction methods. If different construction tools and methods are used for production piles the above parameters will not be valid.

The developed load-settlement curve was used basically for settlement estimation at the service limit state as mentioned above.

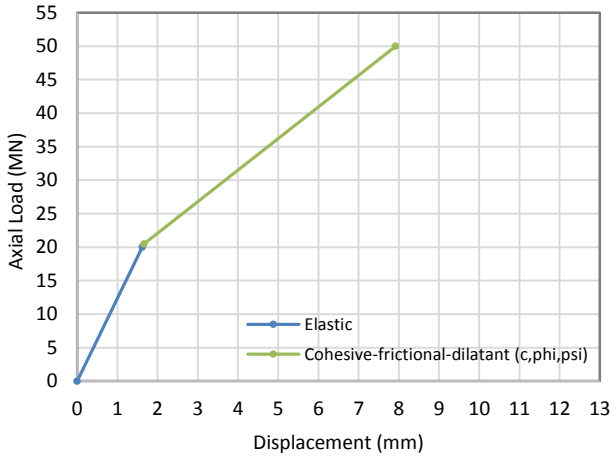

Figure 9. Normalized load-displacement relationship for limestone (DM)

9 CONCLUSIONS

The load tests of the drilled shaft in limestone and in dolomite provided measurements of relatively high values of side and base resistance for the test shafts. The side and base resistance exceeded the capacity of the loading system, and nominal strength values were not mobilized during the test. A back analysis of the measured side resistance suggested values of the empirical parameter C in the range between 0.82 and 0.92. However, considering the ultimate resistance was not attained, the relationships provided in the current FHWA guidelines and AASHTO appear to be reasonable with respect to estimating side resistance of drilled shafts in hard rock. The load tests showed the load transferred to the tip was somehow larger than that predicted by Pells and Turner approach that is adopted in the CFEM and closer to the closed form solution proposed by Kulhawy and Carter.

An equivalent top load-settlement curve obtained from the load test results was constructed and then calibrated to the Kulhawy and Crater model in order to find the design parameters for the full slip zone.

In summary, the use of the load test results on this project provided verification of the design and significant saving on the total socket length.

10 ACKNOWLEDGMENT

The authors would like to thank the Design-Build Joint Venture (JV) team NouvLR for accepting our proposal for lateral load tests. We are also grateful to the Caisse de Dépôt et Placement du Québec (CDPQ) for authorizing the publication of the load test results.

11 REFERENCES

American Association of State Highway and Transportation Officials (2017), *AASHTO LRFD Bridge Design Specifications*.

Brown, D.A., (2008). "*Load Testing of Drilled Shaft Foundations in Limestone, Nashville, TN.*" Research Report for ADSC – Southeastern Chapter.

Brown, D.A., Turner, J.P, and Castelli, R.J., (2010). *Drilled Shafts: Construction Procedures and LRFD Design Methods*. FHWA NHI-10-016, May 2010.

Canadian Foundation Engineering Manual, 4th edition, Canadian Geotechnical Society 2006.

Carter, J.P. and F.H. Kulhawy, "*Analysis and Design of Drilled Shaft Foundations Socketed into Rock*," Report EL-5918, Electric Power Research Institute, Palo Alto, Calif., 1988, 188 pp.

Horvath, R.G. and Kenney, T.C., (1979). "*Shaft Resistance of Rock Socketed Drilled Piers*." Proceedings, Symposium on Deep Foundations, ASCE, New York.

Kulhawy, F.H. and J.P. Carter, "*Settlement and Bearing Capacity of Foundations on Rock Masses*" In Engineering in Rock Masses, F.G. Bell, Ed., Butterworth–Heinemann, Oxford, England, 1992a, pp. 231–245.